articles articles search
toc previous next author subject form home alpha

Journal of the Brazilian Society of Mechanical Sciences
Print version ISSN 0100-7386

J. Braz. Soc. Mech. Sci. vol.24 no.3 Rio de Janeiro July 2002

http://dx.doi.org/10.1590/S0100-73862002000300001

Instabilities in electrochemical systems with a rotating disc electrode

J. Pontes[I]; N. Mangiavacchi[II]; A. R. Conceição[III]; O. R. Mattos[III]; O. E. Barcia[IV]; B. Tribollet[V]

[I]Metallurgy and Materials Engineering Department EE/COPPE/UFRJ PO Box 68505 21945-970 Rio de Janeiro, RJ. Brazil E-mail: jopontes@ufrj.br
[II]Institute of Mathematical and Computational Sciences USP-S. Carlos PO Box 668 13560-161 S.Carlos, SP. Brazil E-mail: norberto@icmc.sc.usp.br
[III]Metallurgy and Materials Engineering Department EE/COPPE/UFRJ PO Box 68505 21945-970 Rio de Janeiro, RJ. Brazil E-mail: anderson@metalmat.ufrj.br / omattos@metalmat.ufrj.br
[IV]Institute of Chemistry - UFRJ PO Box 68505 21945-970 Rio de Janeiro, RJ. Brazil E-mail: barcia@metalmat.ufrj.br
[V]UPR15 - CNRS, Physique des Liquides et Electrochimie 4 place Jussieu, 75252 Paris Cedex 05, France E-mail: bt@ccr.jussieu.fr

Services on Demand

Article

ReadCube
Article in xml format
Article references
How to cite this article
Curriculum ScienTI
Automatic translation
Send this article by e-mail

Indicators

Cited by SciELO
Access statistics

Related links

Share

More
More

Permalink

ABSTRACT

Polarization curves experimentally obtained in the electro-dissolution of iron in a **1 M H_2SO_4** solution using a rotating disc as the working electrode present a current instability region within the range of applied voltage in which the current is controlled by mass transport in the electrolyte. According to the literature (Barcia et. al., 1992) the electro-dissolution process leads to the existence of a viscosity gradient in the interface metal-solution, which leads to a velocity field quantitatively different form the one developed in uniform viscosity conditions and may affect the stability of the hydrodynamic field. The purpose of this work is to investigate whether a steady viscosity profile, depending on the distance to the electrode surface, affects the stability properties of the classic velocity field near a rotating disc. Two classes of perturbations are considered: perturbations monotonically varying along the radial direction, and perturbations periodically modulated along the radial direction. The results show that the hydrodynamic field is always stable with respect to the first class of perturbations and that the neutral stability curves are modified by the presence of a viscosity gradient in the second case, in the sense of reducing the critical Reynolds number beyond which perturbations are amplified. This result supports the hypothesis that the current oscillations observed in the polarization curve may originate from a hydrodynamic instability.

Keywords: Rotating disc flow, electrochemical instabilities, hydrodynamic stability, turbulence

Introduction

Polarization curves experimentally obtained in the electro-dissolution of iron in a **1 M H_2SO_4** solution using a rotating disc as the working electrode present three different regions (Barcia et. al., 1992). The first region is associated with low overvoltages applied to the working electrode and the current is a function of the electric potential and dissolution process only. The electric current is controlled by the transfer of charges at the interface rotating disc/electrolyte solution, and the mass transport does not affect the electro-dissolution process. By increasing the applied potential, the curves show a second region where the hydrodynamic conditions, which depend on the angular velocity imposed to the rotating disc electrode, affect the rate of the anodic dissolution of iron. The current is a function both of the applied potential and the hydrodynamic field developed close to the rotating electrode. By further increasing the applied overvoltage a third region appears, where the current is totally controlled by mass-transport processes. In this third region, polarization curves present a current plateau, defining a limit value for the current, which depends on the hydrodynamic conditions set by the angular velocity of the electrode.

Two current instabilities are observed in the third region: one at the beginning of the current plateau and a second one at the end, where the electrode surface undergoes an active to passive transition (Ferreira et. al., 1994). The first instability is intrinsic to the system, while the current instability close to the active-passive transition is affected by the output impedance of the control equipment. This instability can be suppressed by using a negative feedback resistance (Epelboin, 1972), that gives rise to continuous curves.

Most explanations presented in the literature for the current instabilities are based on mechanisms proposing a **$FeSO_4$** film precipitated at the electrode surface (Russel and Newman, 1986). In fact, changes in the ohmic voltage drop due to precipitation and dissolution of a **$FeSO_4$** film, coupled with the output impedance of the control equipment, provide an acceptable explanation for the instability observed in the active/passive transition region. However, this model can not be generalized to explain oscillations observed at the beginning of the current plateau. By using electro-hydrodynamic (EHD) impedance measurements, Barcia et. al. (1992) studied the electro-dissolution of iron electrodes in **1 M H_2SO_4** at the current plateau before and after the first instability region. EHD impedance is a non-stationary technique which introduces a perturbation with variable frequency and low amplitude in the angular velocity of the rotating disc electrode (Tribollet and Newman, 1983). This perturbation affects the hydrodynamic and mass boundary layers, the mass transfer process and, consequently, the current response at constant applied overvoltage. Analysis of the EHD impedance results provides information on the state of the electrode surface. In particular it gives information on whether the surface is partially blocked (Caprani, 1987), uniformly accessible or covered by a porous film (Deslouis, 1987). Barcia et. al. (1992) verified that the electrode surface is uniformly accessible before and after the first current instability, showing that the surface is not covered by a film. In these conditions it is highly improbable that the electro-dissolution kinetics leads to the deposition of a film in the beginning of the first instability region and that this film disappears at the end of that region, in order to restore the steady-state current at the same level observed before the onset of the instability. Moreover, Barcia et. al. (1992) propose that the electro-dissolution process leads to the existence of a viscosity gradient in the diffusion boundary layer, which could affect the stability of the hydrodynamic field and explain the observed current instability. The purpose of this paper is to investigate the influence a viscosity gradient on the stability of the steady flow. The classic rotating disc flow, modified by the existence of a viscosity gradient pointing along the axial direction, is assumed as the steady hydrodynamic field close to the electrode and a linear stability analysis of this solution is performed, considering two classes of perturbations.

The existence of a hydrodynamic instability in rotating disc flow has been the object of a number of investigations, both experimental and theoretical in the case of fluids with uniform viscosity. The main result shows that the steady flow becomes unstable beyond a certain nondimensional distance from the axis of rotation. This distance is the *Reynolds number* of the problem, defined by:

$$R = r\left(\frac{\Omega}{\nu(\infty)}\right)^{1/2} \qquad (1)$$

where r is the radial distance from the axis, W and n (¥) are the angular velocity and the bulk viscosity far from the disc surface.

The flow develops corotating vortices which spiral outward with their axes along logarithmic spirals of angle 90º + $\varepsilon(\varepsilon \approx 13^\circ)$ with respect to radius of the disc. The first study of transition on a rotating disc, due to Smith (1946), found sinusoidal disturbances in the boundary layer. Subsequently, Gregory, Stuart & Walker (1955) found stationary vortices at nondimensional radii varying from R = 427 to 530, in a flow visualization using the wet-china-clay technique. The experimental critical value of **R** found in the literature, below which all small disturbances dampen, has been reported as being anywhere between 182 and 530. As pointed out by Wilkinson & Malik (1985), "the discrepancy between the values of critical Reynolds number obtained from hot-wire studies and the earlier relatively high values obtained by visual techniques clearly results from the insensitivity of visual techniques to very small disturbances".

Malik (1986) determined the neutral stability curve for stationary vortex disturbances, which turn with the same angular velocity than the disc. The neutral curve was obtained through a linear stability analysis, in which viscosity, streamline curvature and Coriolis forces effects were taken into account. Neutral curves are presented in á x R, â x R and e x R planes for zero-frequency disturbances, where a and b are the components of the real perturbation wavevector along the radial and azimutal directions and e is the tangent of the angle between the perturbation and the radial direction, given by e = a/b. The critical Reynolds number was found to be in good agreement with experimental results, at a value of R = 285.36.

A comprehensive review of the literature on the subject, concerning research made until 1989 can be found in the paper by Reed and Saric (1989).

Faller (1991) addressed the problem of spiral vortices turning with angular velocity different from the disc velocity and found a critical Reynolds number of 69.4 for vortices with a negative wave angle of –19.0º and turning with an angular velocity smaller than the disc velocity.

Lingwood (1995) presented the neutral curve for vortices turning with several angular velocities and theoretical results concerning the asymptotic response of the flow to an impulsive excitation exerted in the flow at a certain radius in t = 0. In this case the wavenumber component along the radial direction, a, was assumed to be complex, leading to an exponential growth along that direction. The neutral curve for this case defines the region of absolute instability, with a critical Reynolds number of R = 510.625.

We emphasize that all these results refer to constant viscosity fluids and the current instabilities observed in the electrochemical experiments conducted in our group occur with Reynolds numbers of order of 50, which is a figure below critical values reported in the literature for rotating disc flow. Hydrodynamic instabilities in this range of Reynolds numbers, if they exist, are possibly due to reasons not taken into account in those studies. One possible reason is nonconstant viscosity, which is considered in this paper.

To investigate the importance of the hydrodynamics in the electro-dissolution of iron, Ferreira (1993) and Geraldo (1998) studied the influence of the viscosity on the current oscillations observed at the beginning of the current plateau region measured in electrochemical cells where the working electrode consists of a rotating disc. These authors found that increasing the electrolyte viscosity - and therefore decreasing the Reynolds number - by adding glycerol to the solution, forces the current oscillations to a periodic behavior or even suppresses the instability. The facts that no hydrodynamic instability is observed in the range of Reynolds numbers of the experiments for the case of constant viscosity, and that a viscosity gradient has been observed in the boundary layer in the electrochemical cells, suggest that the viscosity gradient may play an important role in the hydrodynamic stability of the flow and affect therefore the electric current.

In this work we perform a linear stability analysis to investigate the influence of a viscosity gradient along the axial direction, on the stability of the boundary layer developed close to the rotating disc electrode. In order to avoid the difficulties of evaluating the steady hydrodynamic and concentration fields and performing a stability analysis of the coupled fields we shall adopt the strategy of assuming a steady viscosity profile, dependent on the axial direction.

Two classes of axisymmetric perturbations are considered. The first one consists of perturbations with a structure close to the structure of the base state, with no periodic variations along the radial or azimutal directions. In the second class, a real wavevector with wavenumber a, pointing in the radial direction is assumed.

A small perturbation is added to the steady-state hydrodynamic field and the evolution of the perturbed field is investigated with the appropriate linearized form of the evolution equations. Space derivatives are discretized transforming the original formulation in a generalized eigenvalue/eigenvector problem. The eigenvectors contain a description of each perturbation mode in the points of the grid. The sign of the real part of the associated eigenvalue defines the stability of the mode and the imaginary part determines the natural frequency of the mode. The problem is solved numerically.

Some preliminary results concerning this same analysis were presented by Pontes et. al (2000a, b) but the effect

of variable viscosity was masked by inaccuracies in the computation of the neutral curves presented by those authors. The paper is organized as follows: Next section presents the evolution equations governing the base state, the assumed viscosity profiles and the steady-state solution of the problem for both constant and variable viscosity fluids. Subsequent sections present the temporal linear stability analysis of the hydrodynamic field with respect to the first, the second class of perturbations considered and the conclusions.

The Base State

In this section we describe the base state of the problem, which is assumed as the steady hydrodynamic field near a rotating disc with large diameter. This hydrodynamic field is given by the steady-state solution of Eqs.(2-5), which are the continuity and Navier-Stokes equations neglecting all space derivatives along the azimutal direction and assuming uniform pressure along the radial direction (Schlichting, 1968). Additionally, we assume that the viscosity is a function of the axial coordinate z.

$$\frac{\partial v_r}{\partial r} + \frac{v_r}{r} + \frac{\partial v_z}{\partial z} = 0 \tag{2}$$

$$\frac{\partial v_r}{\partial t} + v_r \frac{\partial v_r}{\partial r} - \frac{v_\theta^2}{r} + v_z \frac{\partial v_r}{\partial_z} = -\frac{1}{\rho}\frac{\partial \rho}{\partial r} + \\ + \nu\left(\frac{\partial}{\partial r}\left(\frac{1}{r}\frac{\partial}{\partial r} r v_r\right) + \frac{\partial^2 v_r}{\partial z^2}\right) + \frac{\partial \nu}{\partial z}\left(\frac{\partial v_z}{\partial r} + \frac{\partial v_r}{\partial z}\right) \tag{3}$$

$$\frac{\partial v_\theta}{\partial t} + v_r \frac{\partial v_\theta}{\partial r} + \frac{v_r v_\theta}{r} + v_z \frac{\partial v_\theta}{\partial z} = \\ = \nu\left(\frac{\partial}{\partial r}\left(\frac{1}{r}\frac{\partial}{\partial r} r v_\theta\right) + \frac{\partial^2 v_\theta}{\partial z^2}\right) + \frac{\partial \nu}{\partial z}\frac{\partial v_\theta}{\partial z} \tag{4}$$

$$\frac{\partial v_z}{\partial t} + v_r \frac{\partial v_z}{\partial r} + v_z \frac{\partial v_z}{\partial z} = -\frac{1}{\rho}\frac{\partial p}{\partial z} + \\ + \nu\left(\frac{1}{r}\frac{\partial}{\partial r}\left(r\frac{\partial v_z}{\partial r}\right) + \frac{\partial^2 v_z}{\partial z^2}\right) + 2\frac{\partial \nu}{\partial z}\frac{\partial v_z}{\partial z} \tag{5}$$

The steady-state hydrodynamic field for constant-viscosity fluids close to the axis of a rotating disc was first investigated by von Kármán (1921). As a necessary prelude to the following sections we briefly review von Kármán results (Schlichting, 1968).

Introducing in Eqs.(3-5) the dimensionless functions F, G, H and P, defined by:

$$\overline{v}_r = r\Omega F(\xi) \tag{6}$$

$$\overline{v}_\theta = r\Omega G(\xi) \tag{7}$$

$$\overline{v}_z = (\nu(\infty)\Omega)^{1/2} H(\xi) \tag{8}$$

$$\overline{p} = \rho\nu(\infty)\Omega P(\xi) \tag{9}$$

where $\hat{\imath} = z(\dot{U}/\acute{\imath}\ (\infty))^{1/2}$ and W is the angular velocity of the disc. In the case of electrolytes with variable

viscosity we consider that the transport properties depend on ξ only. Consequently von Kármán´s transformations (von Kármán, 1921) given by Eqs.(6-9) can be used. The problem for variable density and viscosity fluids was studied by Pollard and Newman (1980). In the present case the density is assumed to be constant. By introducing the dimensionless functions in Eqs.(2-5) we obtain a set of three coupled nonlinear ordinary differential equations for the dimensionless functions F, G and H and a fourth equation for P:

$$2F + H' = 0 \qquad (10)$$

$$F^2 - G^2 + HF' = \frac{\partial}{\partial\xi}\left(\frac{\nu(\xi)}{\nu(\infty)}F'\right) \qquad (11)$$

$$2FG + HG' = \frac{\partial}{\partial\xi}\left(\frac{\nu(\xi)}{\nu(\infty)}G'\right) \qquad (12)$$

$$P' + HH' = 2\frac{\nu'(\xi)}{\nu(\infty)}H' + \frac{\nu(\xi)}{\nu(\infty)}H'' \qquad (13)$$

Boundary conditions for F, G and H are F = H = P = 0, G = 1 when ξ = 0, F = G = H' = 0 when $\xi \rightarrow$ ¥ . Conditions F = 0 and G = 1 in ξ = 0 reflect the non-slip requirement at the electrode surface. In order to integrate the above equations a viscosity profile must be assumed. In this work we use the following profile proposed by Barcia et. al. (1992):

$$\frac{\nu(\xi)}{\nu(\infty)} = \frac{\nu(0)}{\nu(\infty)} + \left(1 - \frac{\nu(0)}{\nu(\infty)}\right)\frac{q^{1/3}}{\Gamma(4/3)}\int_0^{\xi} e^{-q\xi^3}\,d\xi \qquad (14)$$

The parameter q defines the slope of the viscosity profile close to the electrode surface. Fig.1 shows the rotating disc used in the experiments conducted by our group. This electrode consists of a 5 mm diameter iron rod embedded in a 10 mm diameter epoxy resin mold such that only its bottom cross section is allowed to contact the electrolyte. Figure 2 shows the nondimensional viscosity and velocity profiles used in the stability analysis presented in this work. Viscosity profiles with q = 15.0 result in a rapid decay of the viscosity to the bulk value, not changing too much the velocity profiles F, G and H. The axial component of the velocity far from the electrode is practically the same than in the case with constant viscosity and so it is the incoming mass flow approaching the electrode. A decrease in the slope of the viscosity profiles obtained with q = 2.0 increases the deviation of the velocity profiles from the constant viscosity case. The incoming mass flow increases but is not too affected by the n (0)/n (¥) ratio. A further decrease in the value of q to 0.05 affects both the velocity profiles and the incoming mass flow rate, which depends now from the n (0)/n (¥) ratio.

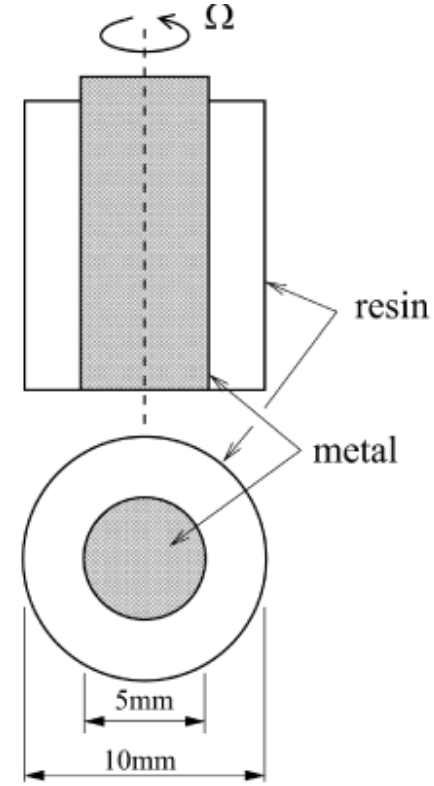

Figure 1. The rotating disc electrode.

Stability with Respect to Perturbations Monotonically Varying Along the Radial Direction

We now address the problem of the stability of the base state with respect to small perturbations in the form:

$$\tilde{v}_r = e^{\omega t} r\Omega f(\xi) \qquad (15)$$

$$\tilde{v}_\theta = e^{\omega t} r\Omega g(\xi) \qquad (16)$$

$$\tilde{v}_z = e^{\omega t} (\nu(\infty)\Omega)^{1/2} h(\xi) \qquad (17)$$

where w is a parameter to be determined. We look for a solution of Eqs. (2-4) in the form of base state plus above perturbations. Since small perturbations are considered, non-linear terms may be neglected leading to the following linearized evolution equations for the perturbations:

$$\left(\frac{1}{r} + \frac{\partial}{\partial r}\right)\tilde{v}_r + \frac{\partial \tilde{v}_z}{\partial z} = 0 \qquad (18)$$

$$\frac{\partial \tilde{v}_r}{\partial t} + \bar{v}_r \frac{\partial \tilde{v}_r}{\partial r} + \tilde{v}_r \frac{\partial \bar{v}_r}{\partial r} - \frac{2\bar{v}_\theta \tilde{v}_\theta}{r} + \bar{v}_z \frac{\partial \tilde{v}_r}{\partial z} + \\ + \tilde{v}_z \frac{\partial \bar{v}_r}{\partial z} = \nu \frac{\partial^2 \tilde{v}_r}{\partial z^2} + \frac{\partial \nu}{\partial z} \frac{\partial \tilde{v}_r}{\partial z} \qquad (19)$$

$$\frac{\partial \tilde{v}_\theta}{\partial t} + \bar{v}_r \frac{\partial \tilde{v}_\theta}{\partial r} + \tilde{v}_r \frac{\partial \bar{v}_\theta}{\partial r} + \frac{\bar{v}_r \tilde{v}_\theta + \tilde{v}_r \bar{v}_\theta}{r} + \bar{v}_z \frac{\partial \tilde{v}_\theta}{\partial z} + \\ + \tilde{v}_z \frac{\partial \bar{v}_\theta}{\partial z} = \nu \frac{\partial^2 \tilde{v}_\theta}{\partial z^2} + \frac{\partial \nu}{\partial z} \frac{\partial \tilde{v}_\theta}{\partial z} \qquad (20)$$

The above equations were derived based on the assumption that the pressure varies along the axial direction, but not along r and that all derivatives with respect to the azimutal coordinate vanish. Consequently, the continuity, the v_r and v_q equations of v_z are decoupled from the equation of v_z so we can drop this last one. The expressions of the base state and of the perturbations are then inserted in the linearized evolution equations. By defining the non-dimensional viscosity as $\nu^* = \nu(\hat{\imath})/\nu(\infty)$ and dropping the asterisk from the new variable we obtain:

$$2f + h' = 0 \qquad (21)$$

$$\nu f''' + \nu' f' - Hf' - 2Ff + 2Gg - F'h = \frac{\omega}{\Omega} F \qquad (22)$$

$$-2Gf + \nu g'' + \nu' g' - Hg' - 2Fg - G'h = \frac{\omega}{\Omega} g \qquad (23)$$

Variables f, f' and f" may be eliminated by replacing:

$$f = -\frac{h'}{2} \qquad f' = -\frac{h''}{2} \qquad f'' = -\frac{h'''}{2}$$

We arrive at a two-equation system, one containing third-order space derivatives and the other one with second-order space derivatives in the form:

$$\begin{pmatrix} \nu D^3 + (\nu' - H)D^2 - 2FD + 2F'; -4G \\ GD - G'; \nu D^2 + (\nu' - H)D - 2F \end{pmatrix} \begin{pmatrix} h \\ g \end{pmatrix} = \frac{\omega}{\Omega} \begin{pmatrix} D & 0 \\ 0 & 1 \end{pmatrix} \begin{pmatrix} h \\ g \end{pmatrix} \qquad (24)$$

where $D^n = d^n/d\xi^n$. Eq. (24) defines a generalized eigenvalue/eigenfunction problem. The eigenfunctions are the normal modes of the model, the real and the imaginary parts of each eigenvalue being the rate of growth and frequency of the associated mode.

The sole parameters appearing in this eigenvalue/eigenfunction problem are those associated with the viscosity profile, n (0)/n (¥) ratio and q (see Eq. 14) which define the slope of the profile close to the electrode surface. No Reynolds number exists for this problem. Boundary conditions of the problem require non-slip flow and vanishing axial component of the velocity at the electrode surface. These conditions are already fulfilled by the base-state, so the hydrodynamic field cannot be modified by the perturbation at the electrode surface. In consequence we must require f = g = h = 0 at $\xi = 0$. Moreover, we conclude from Eq. (21) that h' = 0 at the electrode surface. At $\xi \to$ ¥ we require that the perturbation vanishes (g = h = 0). The generalized eigenvalue/eigenfunction problem is solved numerically. Space derivatives are represented by the following second-order discrete formulae, transforming the original problem in an eigenvalue/eigenvector problem.

$$X_{i+1/2} = \frac{1}{2}(X_i + X_{i+1})$$

$$X'_{i+1/2} = \frac{1}{Äî}(-X_i + X_{i+1})$$

$$X''_{i+1/2} = \frac{0.5}{Äî^2}(X_{i-1} - X_i - X_{i+1} + X_{i+2})$$

$$X'''_{i+1/2} = \frac{1}{Äî^3}(-X_{i-1} + 3X_i - 3X_{i+1} + X_{i+2})$$

The problem is solved using the **LAPACK** double precision *dgegv* routine for real generalized nonsymmetric eigenproblems.

Results

The results of the linear stability analysis are shown in Figs.(3) and (4).

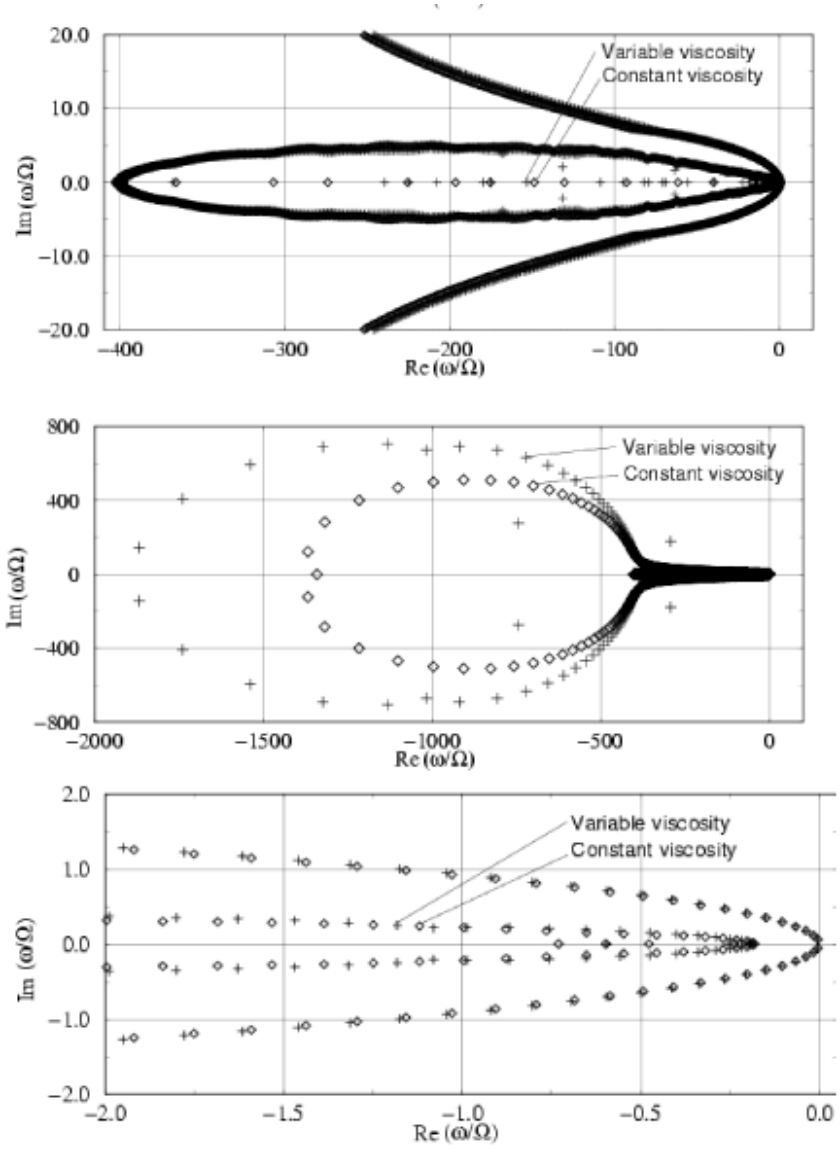

Figure 3. On top: full spectra of eigenvalues for constant and variable viscosity cases. The following two diagrams show successive zooms of first line, focusing eigenvalues with larger real part.

Figure (3) shows the eigenvalues spectra associated to the cases of constant viscosity and variable viscosity, with n = 6.0 and q = 15.0. Spectra obtained for other viscosity profiles are similar to the ones presented in this paper and are not shown here. The spectra are presented in the form of three diagrams containing Â (w /W) x Á (w /W). The diagram shown on top of Fig.(3) contains the full spectra of eigenvalues and the following two show successive zooms of eigenvalues with larger real part. All eigenvalues have negative real parts, indicating that this class of perturbation is always damped.

Figure (4) presents the eigenfuctions obtained for the variable viscosity case with n (0)/n (¥) = 6.0, q = 15, in a system with length ξ = 25 and using a grid with 501 uniformly spaced points. Results obtained for the constant viscosity case and for other viscosity profiles are practically equal to those presented.

Stability with Respect to Perturbations Periodically Modulated Along the Radial Direction

We now address the problem of the stability of the base state with respect to small perturbations periodically modulated along the radial direction, in the form:

$$\tilde{v}_r = e^{\omega t + i\alpha r}\left(\nu(\infty)\Omega\right)^{1/2} f(\xi) \qquad (25)$$

$$\tilde{v}_\theta = e^{\omega t + i\alpha r}\left(\nu(\infty)\Omega\right)^{1/2} g(\xi) \qquad (26)$$

$$\tilde{v}_z = e^{\omega t + i\alpha r}\left(\nu(\infty)\Omega\right)^{1/2} h(\xi) \qquad (27)$$

where a is the perturbation wavenumber along the radial direction and w is the sought eigenvalue of the problem. We look for a solution of the hydrodynamic equations in the form of a base state plus perturbations. By eliminating the pressure, neglecting non-linear terms and all derivatives with respect to the azimutal coordinate q we arrive at a system of three linearized equations for the perturbations, in the form:

$$\left(\frac{1}{r}+\frac{\partial}{\partial r}\right)\tilde{v}_r+\frac{\partial\tilde{v}_z}{\partial z}=0 \qquad (28)$$

$$\frac{\partial}{\partial t}\left(\frac{\partial\tilde{v}_r}{\partial z}-\frac{\partial\tilde{v}_z}{\partial r}\right)+\frac{\partial\bar{v}_r}{\partial z}\frac{\partial\tilde{v}_r}{\partial r}+\frac{\partial\tilde{v}_r}{\partial z}\frac{\partial\bar{v}_r}{\partial r}+\bar{v}_r\frac{\partial^2\tilde{v}_r}{\partial r\partial z}+$$
$$\tilde{v}_r\frac{\partial^2\bar{v}_r}{\partial r\partial z}-\frac{2\bar{v}_\theta}{r}\frac{\partial\tilde{v}_\theta}{\partial z}-\frac{2\tilde{v}_\theta}{r}\frac{\partial\bar{v}_\theta}{\partial z}+\frac{\partial\bar{v}_z}{\partial z}\frac{\partial\tilde{v}_r}{\partial z}+$$
$$\frac{\partial\tilde{v}_z}{\partial z}\frac{\partial\bar{v}_r}{\partial z}+\bar{v}_z\frac{\partial^2\tilde{v}_r}{\partial z^2}+\tilde{v}_z\frac{\partial^2\bar{v}_r}{\partial z^2}-\frac{\partial\bar{v}_r}{\partial r}\frac{\partial\tilde{v}_z}{\partial r}-$$
$$\bar{v}_r\frac{\partial^2\tilde{v}_z}{\partial r^2}-\frac{\partial\tilde{v}_z}{\partial r}\frac{\partial\bar{v}_z}{\partial z}-\bar{v}_z\frac{\partial^2\tilde{v}_z}{\partial r\partial z}=$$

$$\frac{d^2\nu}{dz^2}\left(\frac{\partial\tilde{v}_z}{\partial r}+\frac{\partial\tilde{v}_r}{\partial z}\right)+\frac{d\nu}{dz}\left(-\frac{\tilde{v}_r}{r^2}+\frac{1}{r}\frac{\partial\tilde{v}_r}{\partial r}+\frac{\partial^2\tilde{v}_r}{\partial r^2}+2\frac{\partial^2\tilde{v}_r}{\partial z^2}-\frac{\partial^2\tilde{v}_z}{\partial r\partial z}\right)+$$
$$+\nu\left(-\frac{1}{r^2}\frac{\partial\tilde{v}_r}{\partial z}+\frac{1}{r}\frac{\partial^2\tilde{v}_r}{\partial r\partial z}+\frac{\partial^3\tilde{v}_r}{\partial z\partial r^2}+\frac{\partial^3\tilde{v}_r}{\partial z^3}+\right.$$
$$\left.+\frac{1}{r^2}\frac{\partial\tilde{v}_z}{\partial z}-\frac{1}{r}\frac{\partial^2\tilde{v}_z}{\partial r^2}-\frac{\partial^3\tilde{v}_z}{\partial r^3}-\frac{\partial^3\tilde{v}_z}{\partial r\partial z^2}\right) \qquad (29)$$

$$\frac{\partial\tilde{v}_\theta}{\partial t}+\bar{v}_r\frac{\partial\tilde{v}_\theta}{\partial r}+\tilde{v}_r\frac{\partial\bar{v}_\theta}{\partial r}+\frac{\bar{v}_r\tilde{v}_\theta+\tilde{v}_r\bar{v}_\theta}{r}+\bar{v}_z\frac{\partial\tilde{v}_\theta}{\partial z}+$$
$$+\tilde{v}_z\frac{\partial\bar{v}_\theta}{\partial z}=\nu\left(-\frac{\tilde{v}_\theta}{r^2}+\frac{1}{r}\frac{\partial\tilde{v}_\theta}{\partial r}+\frac{\partial^2\tilde{v}_\theta}{\partial r^2}+\frac{\partial^2\tilde{v}_\theta}{\partial z^2}\right)+\frac{d\nu}{dz}\frac{\partial\tilde{v}_\theta}{\partial z} \qquad (30)$$

We define again the non-dimensional viscosity as n * = n (ξ)/n (¥) and drop the asterisk from the new variable. By inserting the expressions of the perturbations in the continuity equation we obtain an expression for the variable f in the form:

$$f=-\frac{r}{1+i\alpha r}h'$$

The above equation shows that the perturbation variables are not strictly separable, since f actually depends on r. However, this dependency is weak for ar > > 1.

We insert now the expressions for the base state, the perturbations, and for f in eqs.29-29, and arrive at the following two equation system, one containing fourth-order space derivatives and the other one with second-order space derivatives:

$$\begin{pmatrix} a_4D^4+a_3D^3+a_2D^2+a_1D+a_0\,;\, b_1D+b_0 \\ c_1D+c_0\,;\, d_2D^2+d_1D+d_0 \end{pmatrix}\begin{pmatrix} h \\ g \end{pmatrix}=$$
$$\frac{\omega}{\grave{U}}\begin{pmatrix} q_2D^2+q_0\,; & 0 \\ 0 & ;\quad s_0 \end{pmatrix}\begin{pmatrix} h \\ g \end{pmatrix} \qquad (31)$$

where $D^n = d^n/d\xi^n$ and the coefficients in the above operators are given by:

$$a_4 = \nu \qquad a_3 = 2\nu' - H$$

$$a_2 = -\left(\left(1 + 2\alpha^2 R^2\right)/R^2\right)i + i'' - H' - F + i\left(2\alpha\nu/R - \alpha RF\right)$$

$$a_1 = -\left(\left(1 + 2\alpha^2 R^2\right)/R^2\right)i' + \alpha^2 H + i\left(2\alpha i'/R - \alpha H/R\right)$$

$$a_0 = \alpha^2\left(i'' + \alpha^2\nu + 2F + H'\right) + F'' +$$
$$i\left(\alpha RF'' - \alpha\left(\nu'' + \nu\left(1 + 2\alpha^2 R^2\right)/R^2 + F + H' - \alpha^2 R^2 F\right)/R\right)$$

$$b_1 = -2\,G/R - i\left(2\alpha G\right) \qquad b_0 = -2\,G'/R - i\left(2\alpha G'\right)$$

$$c_1 = 2\,RG/\left(1 + \alpha^2 R^2\right) - i\left(2\alpha R^2\,G/\left(1 + \alpha^2 R^2\right)\right) \qquad c_0 = -RG'$$

$$d_2 = \nu \qquad d_1 = \nu' - H \qquad d_0 = -\left(\left(1 + \alpha^2 R^2\right)/R^2\right)\nu - F + i\left(\alpha\nu/R - \alpha RF\right)$$

$$q_2 = 1 \qquad q_0 = -\alpha^2 + i\alpha/R \qquad s_0 = 1$$

Eq.(31) defines a generalized eigenvalue/eigenfunction problem. The eigenfunctions are the normal modes of the model, the real and the imaginary parts of each eigenvalue being the rate of growth and frequency of the associated mode.

For a given viscosity profile the parameter space of the problem contains two variables, the Reynolds number and the nondimensional wavenumber a, which did not exist in the previous case. The effect of the bulk viscosity v(¥) and angular velocity of the electrode W appear in the definition of the Reynolds number.

Boundary conditions of the problem require non-slip flow and vanishing axial component of the velocity at the electrode surface. These conditions are already fulfilled by the base-state, so the hydrodynamic field cannot be modified by the perturbation at the electrode surface. In consequence we must require g = h = 0 at $\xi = 0$. Moreover, we conclude from Eq.(28) that h' = 0 at the electrode surface. At $\xi \to$ ¥ we require that the perturbation vanishes (g = h = 0) and that h' = 0.

The generalized eigenvalue/eigenfunction problem is solved numerically. Space derivatives are represented by the following discrete formulae transforming the original problem in an eigenvalue/eigenvector problem.

$$X_i' = \frac{1}{2\Delta\xi}\left(-X_{i-1} + X_{i+1}\right)$$

$$X_i'' = \frac{1}{\Delta\xi^2}\left(X_{i-1} - 2X_i + X_{i+1}\right)$$

$$X_i''' = \frac{1}{2\Delta\xi^3}\left(-X_{i-2} + 2X_{i-1} - 2X_{i+1} + X_{i+2}\right)$$

$$X_i'''' = \frac{1}{\Delta\xi^4}\left(X_{i-2} - 4X_{i-1} + 6X_i - 4X_{i+1} + X_{i+2}\right)$$

The problem is solved using the **LAPACK** double precision *zgegv* routine for complex generalized nonsymmetric eigenproblems.

Results

In order to identify unstable regions the parameter space was spanned and the neutral curve associated to constant viscosity fluids and six variable viscosity configurations were evaluated. The parameters assumed for the variable viscosity cases are q = 15, 2, and .05 and n (0)/n (¥) = 6 and 12. The resulting nondimensional viscosity and velocity profiles F, G and H are shown in Fig. 2. In all simulations the system length was assumed as ξ_{max} = 10 and the eigenvalue/eigenvector problem was solved in the nodes of a grid containing 201 uniformly spaced points. The results are presented in the form of three neutral stability diagrams, shown in Fig. (5). Each diagram

contains the neutral curve associated to constant viscosity fluids (curve No. 1) and two curves obtained with n(0)/n (¥) = 6 (curve No. 2) and n (0)/n (¥) = 12 (curve No. 3). The diagrams differ by the value of the parameter q, which defines the slope of viscosity profiles close to the electrode surface. Values assumed for q are: 15 for the diagram on top of Fig. 5 (a), 2 for the diagram in the middle (b) and 0.05 for the diagram on bottom of the figure (c). The two hydrodynamic parameters of the problem, namely the Reynolds number and the non-dimensional wavenumber a are represented in the horizontal and vertical axes of this diagram, respectively. The form of the diagram shown in Fig.(5) is similar to those obtained in stability analysis of boundary layers velocity profiles with an inflexion point, which have an inviscid instability. The neutral stability curves define the border between stable and unstable regions. At low Reynolds numbers, all wavelengths are linearly stable. Upon increasing the Reynolds number a bifurcation point defined by the critical pair, (R_c, a_c), is eventually attained. Beyond the bifurcation point a range $a_{min} \leq a \leq a_{max}$, of unstable modes exists. All neutral curves shown in Fig.5 contain two distinct branches, with the absolute minimum for the Reynolds number appearing in the lower one.

The approximate Reynolds number R and the corresponding wavenumber a associated to the critical point and the second minimum, located in the upper branch, are summarized in table 1. In all cases, the introduction of variable viscosity leads to a critical Reynolds number smaller than the one associated to constant viscosity fluids. Larger reductions are obtained with smaller slopes of the viscosity profile, which imply in thicker viscosity boundary layers close to the electrode surface, where n decays to the bulk value. The upper branch of the neutral curves is more affected by the viscosity profile. Results obtained with the two sharpest profiles (q = 15 and q = 2) show an increase in the Reynolds number associated with the second minimum, i.e., the upper branch becomes more stable than the same branch obtained for constant viscosity fluids. In both cases the minimum of the upper branch associated with n (0)/n (¥) = 6 occurs for a Reynolds number smaller than the one associated with n (0)/n (¥) = 12.

Table 1. Approximate coordinates of the two minima of the neutral stability curves shown in Fig. 5. R_1 and α_1 refer to the absolute minimum, located in the lower branch of the neutral curves and R_2 and α_2 refer to the second minimum, located in the upper branch.

	$v(0)/v(\infty)$	q	R_1	α_1	R_2	α_2
1	1	-	136	0.24	411	0.39
2	6	0.05	104	0.24	227	0.45
3	6	2	131	0.26	460	0.36
4	6	15	137	0.25	442	0.36
5	12	0.05	105	0.25	267	0.45
6	12	2	134	0.26	495	0.33
7	12	15	139	0.25	444	0.36

By further decreasing the slope of the viscosity profile (q = 0.05) the stabilizing effect observed in the upper branch is reversed, leading to second minima of the Reynolds number which are much smaller than the one observed for constant viscosity fluids. A wider range of wavenumbers becomes unstable for the same Reynolds number above the critical value. And an increase in the viscosity close to the electrode surface, from n (0)/n (¥) = 6 to n (0)/n (¥) = 12 reduces the Reynolds number of the second minima.

Figures 6, 7 and 8 present eigenmodes evaluated in the approximate coordinates of minima of the neutral curves, as given in Table 1. All modes shown in these figures were evaluated in boxes with length ξ_{max}, using numerical grids with 501 points. Figure 6 shows the 20 eigenmodes of constant viscosity fluids, corresponding to eigenvalues with largest rate of growth, Â(l), evaluated in the critical point, R = 136, a = 0.24.

Figure 7. shows the eigenmodes evaluated at the critical point. This figure shows the eigenmodes associated to the eigenvalue with larger rate of growth, for each parameter configuration. Figure 8 is similar to Fig. 7, with eigenmodes evaluated in the second minimum of the neutral curves, given in Table 1.

Figures 6-8 shows that modes of h tend to decay at larger distances from the electrode surface than modes of g. This is particularly true for the mode with the larger rate of growth, shown in Figs. 7 and 8.

Conclusions

In this work we studied how the linear stability of the hydrodynamic field developed close to a rotating disc electrode is affected by the introduction of a viscosity gradient along the rotating axis direction. The steady rotating disc flow was calculated and the stability of the new base flow with respect to two classes of perturbations was studied: perturbations monotonically varying along the radial direction and perturbations periodically modulated along the radial direction.

The results show that the hydrodynamic field is stable with respect to the first class of perturbations for both constant and variable viscosity fluids. The stability problem associated to this class of perturbation does not contain a Reynolds number, which is the bifurcation parameter defining the stability limit in flows.

A totally different situation occurs when perturbations periodically modulated along the radial direction are considered. In this case the operators appearing in the linear stability problem contain two parameters, the Reynolds number and the perturbation wavenumber a and the neutral stability curve drawn in the *R* x a plane is affected by the existence of a viscosity gradient pointing in the axial direction. The curves present two branches, with the absolute minimum for the Reynolds number located in the lower one and a second minimum existing in the upper branch. Introduction of variable viscosity lead, in all parameter configurations studied in this work, to a reduction in the critical Reynolds number. The effect becomes stronger as the slope of the viscosity profile decreases, and leads to a thicker region affected by the viscosity gradient, close to the electrode surface. The critical Reynolds number is not too affected by the n (0)/n (¥) ratio and in all cases, the critical Reynolds obtained with n (0)/n (¥) = 6 was smaller than the one obtained with n (0)/n (¥) = 12, all other parameters having the same value.

The upper branch of the neutral curves is differently affected by a viscosity profile. Sharp slopes lead to an increase in the Reynolds number of the second minimum but this effect is reversed with low slope viscosity profiles.

In summary, the introduction of a viscosity profile affects the stability properties of the steady hydrodynamic field. In all cases considered in this work a reduction in the critical Reynolds number was observed and it is expected that the neutral curves for perturbations containing modulations along the azimutal direction will also be affected.

The Reynolds number attained in the experimental setup used by our group at the Federal University of Rio de Janeiro falls in the range 30-50 and it is known that neutral curves for spiral perturbations modulated along the azimutal direction may have a critical Reynolds number smaller than the ones obtained in the present work. In particular, the neutral curves presented by Lingwood (1995) for vortex structures turning with angular velocity smaller than the disc velocity lead to critical Reynolds numbers of 69.4 and it is not excluded that lower values be attained with variable viscosity fluids. In that case hydrodynamic stability could be on the base of the current instabilities observed in the electro-dissolution of iron rotating disc electrodes.

Acknowledgements

The numerical calculations were done at the High-Performance Computer Center (NACAD-UFRJ) and in the workstations of the Metallurgy and Materials Eng. Dept. (UFRJ). The authors acknowledge fruitful discussions with Profs. R. E. Kelly from the University of California at Los Angeles and D. Walgraef from the Free University of Brussels. J. P. acknowledges also financial support from FAPERJ (Brazil) received under the contract number E-26/171.300/2001

References

Anderson, E., Bai, Z., Bischof, C., Demmel, J., Dongorra, J., Croz, J. D., Greenbaum, A., Hammarling, S., McKenney, A., Ostrouchov, S., and Sorensen, D. *LAPACK User's Guide*. SIAM, Philadelphia, USA, 1995. [Links]

Barcia, O. E., Mattos, O. R., and Tribollet, B. Anodic dissolution of iron in acid sulfate under mass transport control. *J. Eletrochem. Soc*. *139* (1992), 446-453. [Links]

Caprani, A., Desloius, C., Robin, S., and Tribollet, B. Transient mass transfer at partially blocked electrodes. *J. Eletroanal. Chem*. *238* (1987), 67-91. [Links]

Cebeci, T., and Stewartson, K. On stability and transition in three-dimensional flows. *AIAA J*. *18-4* (1980), 398-405. [Links]

Corke, T. C., and Knasiak, K. F. Cross-flow instability with periodic distributed roughness. In *IU-TAM Symposium on Nonlinear Instability and Transition in Three-Dimensional Boundary Layers* (1996), P. W.Duck and P. Hall, Eds., Kluwer, pp. 267-282. [Links]

Desloius, C., Tribollet, B., Duprat, and Moran, F. Transient mass transfer at a coated rotating disc electrode. *J. Eletrochem. Soc*. 134 (1987), 2496-2501. [Links]Epelboin, I., Gabrielli, G., Keddam, M., Lestrach, J. C., and Takenouti, H. Passivation of iron in sulfuric acid medium. *J. Eletrochem. Soc*. *126* (1979), 1632-1637. [Links]

Faller, A. J. Instability and transition of the disturbed flow over a rotating disc. *J. Fluid Mech. 230* (1991), 245-269. [Links]

Ferreira, J. R. R. M., Barcia, O. E., and Tribollet, B. Iron dissolution under mass transport control: the effect of viscosity on the current oscillation. *Eletrochim. Acta 39* (1994), 933-938. [Links]

Geraldo, A. B., Barcia, O. E., Mattos, O. R., Huet, F., and Tribollet, B. New results concerning the oscillations observed for the system iron-sulfuric acid. *Electrochim. Acta 44* (1998), 455-465. [Links]

Gregory, N., Stuart, J. T., and Walker, W. S. On the stability of three-dimensional boundary layers with application to the flow due to a rotating disc. Phil. Trans. Roy. Soc. London A-248 (1955), 155-199. [Links]

Kobayashi, R., Kohama, Y., and Takamadate, C. Spiral vortices in a boundary layer transition regime on a rotating disc. *Acta Mechanica 35* (1980), 71-82. [Links]

Lilly, D. K. On the stability of Ekman boundary flow. *J. Atm. Sci. 23* (1966), 481-494. [Links]

Lingwood, R. J. Absolute instability of the boundary layer on a rotating disc. *J. Fluid Mech. 299* (1995), 17-33. [Links]

Malik, M. R. The neutral curve for stationary disturbances in rotating-disc flow. *J. Fluid Mech*. *164* (1986), 275-287. [Links]

Malik, M. R., Wilkinson, and Orzag, S. A. Instability and transition in a rotating disc. *AIAA J. 19-9* (1981), 1131-1138. [Links]

Podesta, J. J., Piatti, R. C. V., and Arvia, A. J. The potentiostatic current oscillations at iron/sulfuric acid solution interfaces. *J. Eletrochem. Soc. 126* (1979), 1363-1367. [Links]

Pollard, R., and Newman, J. Silicon deposition on a rotating disc. *J. Eletrochem. Soc. 127* (1980), 744-752. [Links]

Pontes, J., Mangiavacchi, N., Barcia, O. E., Mattos, O. R., Tribollet, B., and Walgraef, D. Hydrodynamic stability close to a rotating disc electrode with respect to axisymmetric perturbations. In *Anais da II Escola Brasileira de Primavera Transição e Turbulênfontcia* (Uberlândia, Brazil, 2000), pp. 484-495. [Links]

Pontes, J., Mangiavacchi, N., Barcia, O. E., Mattos, O. R., Tribollet, B., and Walgraef, D. Stability of the hydrodynamic field close to a rotating disc electrode. In *Proceedings of the 8 the Brazilian Congress of Thermal Engineering and Sciences* (Brazil, 2000). Paper S35P31 (in CD). [Links]

Reed, H. L., and Saric, W. S. Stability of three-dimensional boundary layers. *Ann. Rev. Fluid Mech. 21* (1989), 235-84. [Links]

Russel, P., and Newman, J. Current oscillations observed within the limiting current plateau for iron in sulfuric acid. *J. Eletrochem. Soc. 133* (1986), 2093-2097. [Links]

Schlichting, H. *Boundary Layer Theory*. McGraw-Hill, 1968. [Links]

Smith, N. Exploratory investigation of laminar boundary layer oscillations on a rotating disc. Tech. Rep. TN-1227, NACA, Dec. 1946. [Links]

Stewartson, K., and Simpson, C. J. The unsteady boundary layer on a rotating disc in a counter rotating fluid. Part 2. *J. Fluid Mech. 121* (1982), 507-515. [Links]

Tribollet, B., and Newman, J. The modulated flow at a rotating disc electrode. *J. Eletrochem. Soc*. 130 (1983), 2016-2026. [Links]

von Kármán, T., and Angew, Z. Uber laminare und turbulente reibung. *Math. Mec. 1* (1921), 233-252. [Links]

Wilkinson, S., and R., M. M. Stability experiments in the flow over a rotating disc. *AIAA J. 23* (1985), 588. [Links]

All the contents of this journal, except where otherwise noted, is licensed under a Creative Commons Attribution License

ABCM

Av. Rio Branco, 124 - 14. Andar
20040-001 Rio de Janeiro RJ - Brazil
Tel. : (55 21) 2221-0438
Fax.: (55 21) 2509-7128

e-Mail

abcm@domain.com.br